CHEMISTRY OF MATERIALS

Review

pubs.acs.org/cm

Graphene-Based Enhanced Raman Scattering toward Analytical Applications

Na Zhang, Lianming Tong,* and Jin Zhang*

Center for Nanochemistry, Beijing National Laboratory for Molecular Sciences, College of Chemistry and Molecular Engineering, Peking University, Beijing 100871, China

ABSTRACT: Due to the single-molecule sensitivity and the capability of chemical fingerprints recognition, surface-enhanced Raman scattering (SERS) has been an attractive analytical technique used in various fields. However, SERS sensing still suffers from several problems, including the heterogeneous adsorption of molecules on SERS substrates, the spectral fluctuation of molecules, the photo/chemical reactions of molecules in direct contact with metal, and the continuum spectral background originated from fluorescence or photocarbonization. Such problems greatly hinder its practical applications, in particular, in SERS quantification. Graphene, the star of the two-dimensional (2D) materials family, can be used for Raman enhancement, termed as graphene-based surface-enhanced Raman scattering (G-SERS). In this review, we will introduce the discovery of graphene-enhanced Raman scattering (GERS), the chemical enhancement, and its extension to other 2D materials beyond graphene. Then we will concentrate on graphene-based SERS toward analytical applications—from graphene-veiled SERS to G-SERS tape for quantitative analysis.

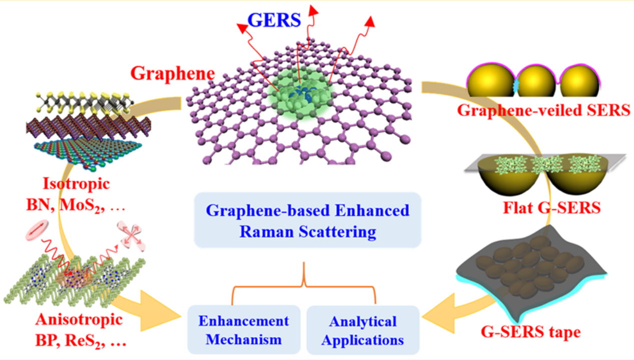

1. INTRODUCTION

Over the years, rapid, precise, and robust analytical methods to detect trace species have been an eternal goal to pursue in many fields, such as environmental monitoring, food safety, and disease diagnosis. Surface-enhanced Raman spectroscopy (SERS), first observed on roughened silver electrodes by Fleischmann et al. in 1974,[1] meets the requirements for its excellent characteristics, such as rapid response, high sensitivity, nondestructive detection, and molecular fingerprint recognition.[2−5]

In spite of the intrinsic low cross section of Raman scattering, SERS can boost the pristine Raman signal by up to 10^8 times.[6] For the typical SERS system, the enhancement consists of electromagnetic and chemical contributions.[2,6−8] The enormous enhancement effect is mainly ascribed to the electromagnetic mechanism (EM), which benefits from the greatly magnified electromagnetic field derived from surface plasmons excited by the incident light.[9,10] The ultrastrong electromagnetic fields usually lie in the roughened spots on the metal surface and in the nanogaps between nanostructures, the so-called "hot spots".[11] The Raman enhancement is roughly proportional to $|E|$,[4] where E is the magnitude of the electromagnetic field enhancement.[9] The chemical mechanism (CM) typically coexists with the EM, but its enhancement factor is only around $10-10^2$ so that the contribution of CM is overwhelmed by that of the EM.[6,12] Anyhow, by virtue of the intervention of surface enhancement, SERS achieves a relatively high sensitivity, even capable of single-molecule detection.[13,14]

However, many problems that hinder the practical application of SERS still remain, which mainly include the following: (1) the spectral fluctuation resulting from the molecular deformation and distortion, particularly under few-molecule-level detection; (2) the chemical bonding induced spectral variation and metal-catalyzed side reactions of the molecules;[15] (3) the laser heating induced photocarbonization of the molecules;[10] and (4) the heterogeneous adsorption of detected molecules at different facets.[14] These years, researchers have made great efforts toward an ideal SERS substrate to overcome the aforementioned drawbacks. Recently, it has been reported that nanoparticles coated with an inert shell can give cleaner enhanced Raman signals, lighting up the alternative of a SERS substrate with a spacer layer, which is thin and chemically inert.[16]

Graphene, the star of the 2D materials family, is a promising candidate to overcome the aforementioned drawbacks of a conventional SERS substrate. Graphene is a monolayer of sp^2 bonded carbon atoms packed into a honeycomb-like crystalline structure. Since its discovery in 2004,[17] graphene has been wildly employed in manifold research fields, from chemical sensors to transistors, for its excellent properties,[18−23] such as unique electron and photon structures, ultrahigh carrier mobility, excellent mechanical property, atomic uniformity, biological compatibility, chemical inertness, and flexibil-

Received: July 17, 2016
Revised: August 31, 2016
Published: September 5, 2016

ity.[17,24,25] Beyond that, graphene can be easily obtained by mechanical exfoliation from HOPG or Kish graphite, and can be clearly identified by optical microscopy on a 300 nm thick SiO_2/Si substrate, which means the superiority of economy and convenience for normal laboratory use.[26−28] Such merits also endow graphene as a splendid candidate as a substrate for Raman enhancement, termed as graphene-enhanced Raman scattering (GERS).[29]

As a new figure of a SERS substrate, graphene is opening up a new way both to study the CM of SERS and to boost the practical application of the SERS technique, which has drawn enormous attention in recent years.[30−32] With the development of GERS, a wave of innovative flat materials, from isotropic hexagonal boron nitride (h-BN) and molybdenum disulfide (MoS_2), to anisotropic orthorhombic black phosphorus (BP) and triclinic rhenium disulfide (ReS_2),[33−37] is following in the wake of graphene, providing new possibilities for both the mechanism study and the practical applications of SERS. In this review, we will introduce the discovery of graphene-enhanced Raman scattering (GERS), the chemical enhancement, and its extension to other 2D materials beyond graphene. Then we will concentrate on graphene-based SERS toward sensing applications—graphene-supported SERS, graphene-veiled SERS, and G-SERS tape for quantitative analysis.

2. GRAPHENE-ENHANCED RAMAN SPECTROSCOPY (GERS)

On the ideal 2D plane of graphene, discarding the metal−molecule contact induced signal disturbances, GERS rewards a valuable analytical tool featured of clean signal, stable response and recyclability. In this part, we will focus on the renaissance of CM-SERS by virtue of graphene. The enhanced Raman scattering by other 2D materials beyond graphene will also be discussed.

2.1. Discovery of GERS. Since the cross section of fluorescence (~10^{-16} cm^2) is much larger than that of Raman scattering (~10^{-22} cm^2),[38] SERS signals of dye molecules severely suffer from the interference of fluorescence. Our group found out that graphene can effectively quench the photoluminescence (PL) of fluorescent dyes (e.g., rhodamine 6G, R6G; and protoporphyrin IX, PPP) adsorbed on graphene, thus enabling clear Raman signals without a wavy fluorescence background (Figure 1b).[39] The PL quenching effect is basically due to electron transfer and energy transfer between graphene and the dye molecules.[40] In fact, clean Raman spectra of fluorescent dyes under resonant excitation are normally difficult to acquire, and graphene serves as an ideal platform to make it easy and effective.

More inspiringly, we observed that graphene can also be used as a substrate to enhance Raman signals of adsorbed molecules (Figure 1a).[29] Systematic experiments were implemented with typical dye molecules used as Raman probes, such as phthalocyanine (Pc), R6G, PPP, and crystal violet (CV) deposited by means of vacuum evaporation or solution soaking. The intensities of the Raman signals of Pc on monolayer graphene were much stronger than those on nongraphene area, indicating that graphene can enhance the Raman signals of these molecules (Figure 1c). This effect is the so-called "graphene-enhanced Raman scattering (GERS)".

2.2. Chemical Mechanism of GERS. As mentioned before, the two widely accepted mechanisms are the electromagnetic mechanism (EM) and chemical mechanism (CM). The EM is a long-range effect, as the electromagnetic field can expand several nanometers normal to the surface, while the CM is a short-range effect which requires the molecule be in contact with the substrate, so that the charge transfer can occur. Thus, CM is usually regarded as a "first layer effect".[8,29] It is believed that the charge transfer leads to the increased polarizability of the molecule and, consequently, increased cross section of Raman scattering. Usually, the enhancement factor (EF) of CM is around or less than 10^2.

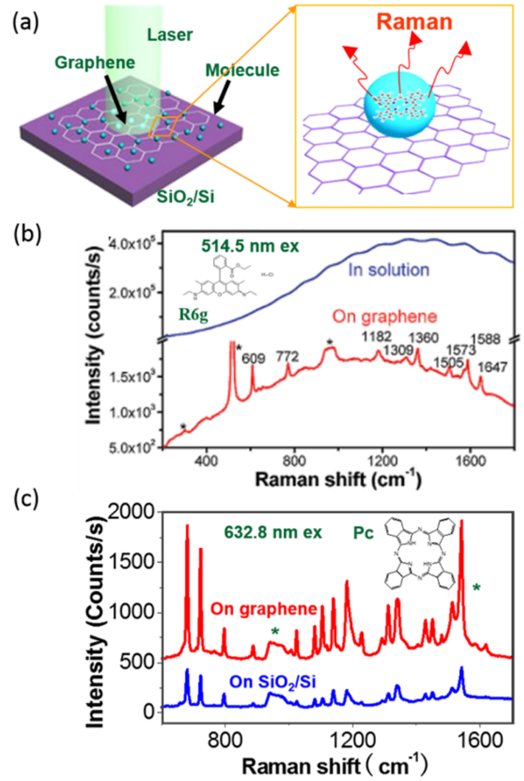

Figure 1. (a) Schematic illustration of the GERS system. (b) Photoluminescence suppression effect of R6G on graphene. The blue line is the spectrum of R6G in solution, and the red line is the spectrum of R6G on graphene. (c) Raman spectra of Pc molecules on monolayer graphene and a blank SiO_2/Si substrate. Adapted with permission from refs 29 and 39. Copyright 2010 and 2009 American Chemical Society.

Ling et al. deposited 1−4 layers of PPP on (upon) graphene by the LB technique, and found out that the first layer PPP on graphene contributed the dominant Raman intensity, which accords with the "first layer effect".[41] The Raman EF of CuPc in the GERS system was 2−17, and it varied with the number of graphene layers.[29] On the other hand, the magnitude of its EF was found to be dependent on the symmetry of the vibrational modes. For Pc molecules, the EF was obtained as follows: A_g (~15 times) > B_{3g} (~5 times) > macrocycle breathing (~2 times). The magnitude of the enhancement and the vibration dependence of the EFs are consistent with the chemical enhancement mechanism. The molecular orientation dependence of GERS was also explored, and CuPc molecules in lying-down and upstanding configurations exhibited different EFs.[42] This result is accessible because the molecules in different molecular orientations on graphene imply different extent of interaction between them. Fermi level modulation of the substrate by imposing gate voltage resulted in the variation of GERS enhancement magnitude.[43,44] Apart from that, GERS enhancement can also be modulated by the energy of incident

DOI: 10.1021/acs.chemmater.6b02925
Chem. Mater. 2016, 28, 6426−6435

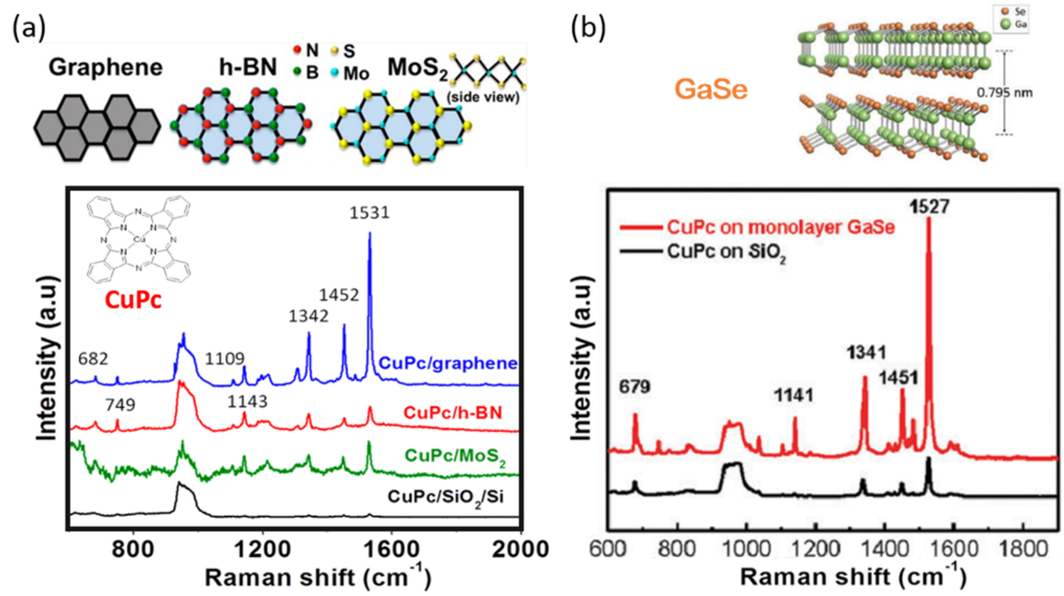

Figure 2. (a) Raman spectra of the CuPc molecule on the blank SiO_2/Si (black line), graphene (blue line), h-BN (red line), and MoS_2 (green line) substrates, respectively. The Raman signal was excited by a 632.8 nm laser. Adapted with permission from ref 35. Copyright 2014 American Chemical Society. (b) Raman spectra of CuPc deposited on a monolayer GaSe (red line) and the SiO_2/Si substrate (black line) under 514 nm excitation. Inset shows the schematic layer structure of GaSe and the thickness of the monolayer. Adapted with permission from ref 47. Copyright 2015 Royal Society of Chemistry.

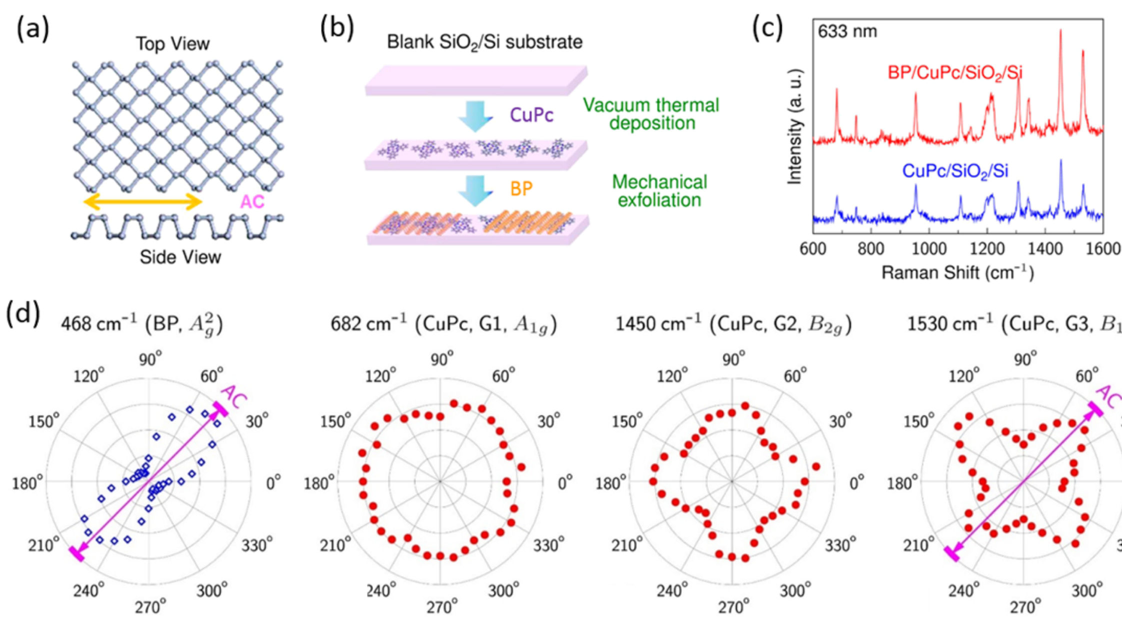

Figure 3. (a) Top and side view of orthorhombic BP. The armchair direction of BP is denoted as AC and marked by the yellow double-arrow. (b) Schematic illustration of sample preparation procedure. (c) Raman spectra of CuPc molecules on a 300 nm SiO_2/Si substrate with (red) and without (blue) few-layer BP on top. (d) Polar plots of the normalized intensities of the 468 cm^{-1} (BP, A_g^2), 682 cm^{-1} (CuPc, A_{1g}), 1450 cm^{-1} (CuPc, B_{2g}), and 1530 cm^{-1} (CuPc, B_{1g}) modes as a function of sample rotation angle measured on BP. The AC direction of BP is marked by the purple double-arrow. Adapted with permission from ref 37. Copyright 2015 American Chemical Society.

laser, and the GERS was proven to be a ground-state charge-transfer mechanism.[45] Graphene-thickness-dependent GERS shows that monolayer and bilayer graphene have different electronic structure and then the different doping effect of the probe molecules, which shifts the Fermi level of graphene differently, leads to different energy band matching with the probe molecules, yielding different chemical enhancement.[46]

2.3. Chemical Enhancement from 2D Materials beyond Graphene. *2.3.1. Isotropic 2D Layered Materials.* The investigation of Raman enhancement has been extended to more 2D layered materials beyond graphene, including hexagonal boron nitride (h-BN) and the transition metal dichalcogenides (TMD) (e.g., molybdenum disulfide (MoS_2)).[33−35] They have structures somewhat similar to graphene but different electronic and surface chemical properties. Ling et al. compared the Raman enhancement effect of CuPc molecules on graphene, h-BN, and MoS_2.[35] It was found that all of these 2D materials showed Raman

DOI: 10.1021/acs.chemmater.6b02925
Chem. Mater. 2016, 28, 6426−6435

enhancement but with different EFs (Figure 2a). The EF on graphene was larger than that on BN for the higher-frequency modes of CuPc, and BN demonstrated the strongest Raman enhancement effect for lower-frequency ones, while the EF of MoS_2 showed superiority in neither frequency region. It was concluded that the chemical enhancement can be attributed to both charge transfer and dipole−dipole coupling contributions. The strong charge transfer interaction between graphene and CuPc as well as the interface dipole−dipole interaction between h-BN and CuPc can induce an increase of the electron transition probability and consequently an enhancement of the Raman signal. As for MoS_2, both the charge transfer and interface dipole interaction are much weaker.

Lee et al. studied the Raman scattering of R6G monolayer adsorbed onto graphene, MoS_2 phototransistors, and tungsten diselenides (WSe_2), and also observed Raman enhancement and ascribed it to the charge transfer between the molecules and materials.[36] They studied the thickness-dependence of the materials. For the R6G on the MoS_2 nanosheet, a single layer provided the maximum Raman enhancement, and the EF value decreased pseudolinearly with the number of layers. By contrast, the Raman enhancement factor of the R6G onWSe_2 reached the maximum values for both the mono- and bilayers, and decreased dramatically as the number of layers increased. They provided qualitative theoretical explanations for these trends based on the electric field enhancement due to interlayer interference and the energy band diagrams of both systems. Quan et al. first carried out a systematic investigation of the Raman enhancement on GaSe flakes by using CuPc as a probe.[47] They found that the Raman signals of CuPc on the monolayer GaSe showed much stronger intensity than that on the SiO_2/Si substrate (Figure 2b), and the relative EF can reach up to 14 and decrease with increasing thickness of the GaSe flake. They attributed the Raman enhancement on GaSe to the chemical mechanism arising from the charge transfer between CuPc and GaSe.

2.3.2. Anisotropic 2D Layered Materials. From the symmetry point of view, the above-mentioned 2D materials are all isotropic, so that the Raman enhancement is regardless of the laser polarization. Nowadays, the emerging anisotropic 2D layered materials, such as ReS_2 and black phosphorus (BP), have attracted great interest due to their characteristic anisotropy. For example, BP with orthorhombic structure (Figure 3a) possesses anisotropic conductivity, photoelectric response, light absorption, fluorescence, and Raman scattering.[48−50] The anisotropic Raman scattering feature enables a rapid and precise method to identify the crystalline orientation of BP layers via angle-resolved polarized Raman spectroscopy (ARPRS).[51] More interestingly, such anisotropic 2D layered materials also showed Raman enhancement effect, and revealed richer information on the charge transfer process than using isotropic ones.[37]

CuPc was chosen as a probe molecule, as its high symmetry of D_{4h} can simplify the system. The molecules were loaded on a blank SiO_2/Si substrate by means of vacuum thermal deposition to ensure the uniformity, and then BP was transferred on the top via mechanical exfoliation (Figure 3b). The Raman signals of CuPc molecules were enhanced by BP compared to that on the blank substrate, with the EF in the range 3−6 (Figure 3c). Especially, the Raman spectra of CuPc molecules on BP exhibited a strong polarization dependence (Figure 3d), which is absent on the SiO_2/Si substrate as well as isotropic graphene and BN substrates, indicating that the anisotropic structure of BP should contribute to the polarization dependence of the enhancement.

Using ARPRS, the angular dependence of the normalized Raman spectra was obtained. Polar plots of the normalized intensities of the 468 cm^{-1} (BP, A_g^2), 682 cm^{-1} (CuPc, A_{1g}), 1450 cm^{-1} (CuPc, B_{2g}), and 1530 cm^{-1} (CuPc, B_{1g}) modes change as a function of sample rotation angle measured on BP. The angles with maximum intensity of the B_{1g} mode of CuPc coincide with the armchair (AC) direction of BP (Figure 3d). Similar results were also observed on triclinic ReS_2. The angles with maximum intensity of the B_{1g} mode of CuPc coincide with the zigzag (ZZ) Re chain direction of ReS_2.

The angular variation of the B_{2g} and B_{1g} modes on BP/ReS_2 coincide with the simulation of a single molecule or well aligned molecules by means of the Raman tensor analysis. However, the molecules were randomly oriented through vacuum thermal deposition. Density functional theory (DFT) calculations showed that, for pristine BP, the charges are uniformly distributed across the surface, but for the CuPc/BP system, the charges in the electronic bands near the Fermi level are redistributed into 1D chains along the AC direction, while, for the graphene surface, the charge distributions remain isotropic with the presence of CuPc. That is, CuPc induced the anisotropic charge distribution in BP, resulting in anisotropic charge interactions and thus anisotropic Raman enhancement. These results not only provide new insights into the chemical mechanism (CM) process in SERS, but also open up new avenues for the possible exploration of the electronic properties of anisotropic 2D layered materials. Furthermore, it might add up to a new dimension in SERS sensing, i.e., the symmetry of the SERS substrate.

3. ENHANCED RAMAN SCATTERING ON 2D LAYERED MATERIALS FOR SENSING

As mentioned, conventional SERS suffers from certain inherent weaknesses for practical sensing applications. For GERS, the atomic flatness and chemically inert surface of graphene guarantee it an ideal choice as a sensing technique. By using a solution soaking approach, the Raman signals from the molecules can be observed even for concentrations as low as 8 × 10^{-10} M for R6G, and 2 × 10^{-8} M for PPP.[29] The concentration is comparable with that used in the conventional SERS experiments.[52,53] This fantastic performance is also partially due to the π−π interaction induced enrichment of molecules and fluorescence quenching on graphene.

Other 2D materials, such as MoS2 and BN, can also be used to detect molecules. Using MoS_2 as the Raman enhancement substrate, Xu et al. recorded the Raman spectra of R6G molecules with concentrations ranging from 10^{-4} M down to 10^{-7} M.[33] Qiu et al. directly synthesized few-layer MoS_2 on a pyramid-Si as SERS substrate, and the limit of detection of both adenosine and cytidine on this substrate can reach 10^{-6} M.[34] Importantly, the linear relationship between the Raman intensity and the concentration of adenosine or cytidine can apply to the bimolecular detection. BN nanosheets only show a very weak G band at 1370 cm^{-1};[54] therefore, the Raman signals of analyte on BN are not interfered with by those from the substrate. BN nanosheet decorated by aqueously dispersed silver nanoparticle has been developed as a reusable and thermal oxidation-resistant SERS device.[55] Atomically thin BN nanosheets have been found to be excellent substrates for noble metal particles enabled SERS, thanks to their good adsorption of aromatic molecules. It has been shown that the BN-AgNPs

DOI: 10.1021/acs.chemmater.6b02925
Chem. Mater. 2016, 28, 6426−6435

substrate exhibited a very strong SERS activity due to the enrichment of 2-mercaptobenzimidazole (MBI) on the Ag surface through the S and N atoms,[56] offering great potential application in molecular sensors.

4. BOOSTING GERS WITH METAL NANOSTRUCTURES

As the EM enhancement is remarkably higher than CM, metal nanoparticles (gold or silver) can be used to improve the sensitivity of GERS. In this section, we will introduce the strategy of hybrid SERS substrate made up of graphene and metal nanostructures to improve the SERS enhancement. Changing its relative location to the metal nanostructures/probe molecules, graphene varies the role from a supporter to an isolated layer, apart from its initial function as a chemical enhancer. By this means, the virtues of GERS can be fully exploited while the Raman enhancement is dominated by the sizable EM derived from metal nanostructures.

4.1. Graphene-Supported SERS. Metal nanoparticles (gold or silver) can be used to improve the SERS intensity by deposition onto graphene film to form a hybrid SERS substrate, in which graphene acts as a supporter and molecular enricher. In these systems, EM is the dominant contributor with CM adding another order of magnitude to the large SERS enhancement factor. Nanocomposites of the gold or silver (or alloy of both) nanoparticles and graphene or graphene derivatives have been fabricated, and size-controlled nanoparticles have also been designed to gain excellent SERS performance.[30,57−61] For example, Kim et al. used single nanowires on graphene (SNOG) as an efficient, reproducible, and stable SERS-active platform.[62] Leem et al. achieved a 3D crumpled graphene−Au NPs hybrid structure by the delamination and buckling of graphene on a thermally activated, shrinking polymer substrate, which exhibited at least 1 order of magnitude higher SERS detection sensitivity than that of conventional flat graphene−Au NPs.[63]

Composites of graphene and metal as hybrid SERS substrate open up new opportunities in developing and revolutionizing the applications of graphene in biomedical diagnostics, pesticide-residues analysis in agricultural products and environments, as well as biological sensing and imaging.[64−70] For example, Kanchanapally et al. reported the graphene-oxide attached gold nanocage assembly for trace level label-free detection of RDX and TNT nitro explosives, with detection limits as low as 10 fM for TNT and 500 fM for RDX.[71]

It has been widely accepted that, besides the EM enhancement, the improvement of the SERS activity of graphene-metal nanoparticle-hybrid substrate is also a result of their high adsorption ability, strong fluorescence quenching, and additional CM-based SERS effect. However, Lu et al. indicated that the p-doping of graphene in R6G/AuNP/graphene substrate is the dominant factor contributing to the observed high SERS sensitivity, through enhanced molecule adsorption and nonresonance molecular substrate chemical interaction.[72]

4.2. Graphene-Veiled SERS. For a GERS substrate, the absence of metal rules out the metal−molecule contact induced variations of the Raman spectra; however, it compromises a considerable detection sensitivity. In order to retain the superior enhancement of metal nanostructures and simultaneously get rid of the spectral disturbances, many passivated substrates with a thin and pinhole-free coating layer have been exploited. A typical example is the shell-isolated nanoparticles enhanced Raman scattering developed by Tian's group,[16,73] but it is a very delicate technique to get a pinhole-free coating layer with a very small thickness. Graphene, possessing the unique structure of atomic thickness and compact surface, is an ideal candidate material for the spacer layer.

Our earlier work provided a "two-step" approach to prepare an active, graphene-veiled gold substrate, as illustrated in Figure 4a.[74] Mechanically exfoliated graphene was transferred onto an

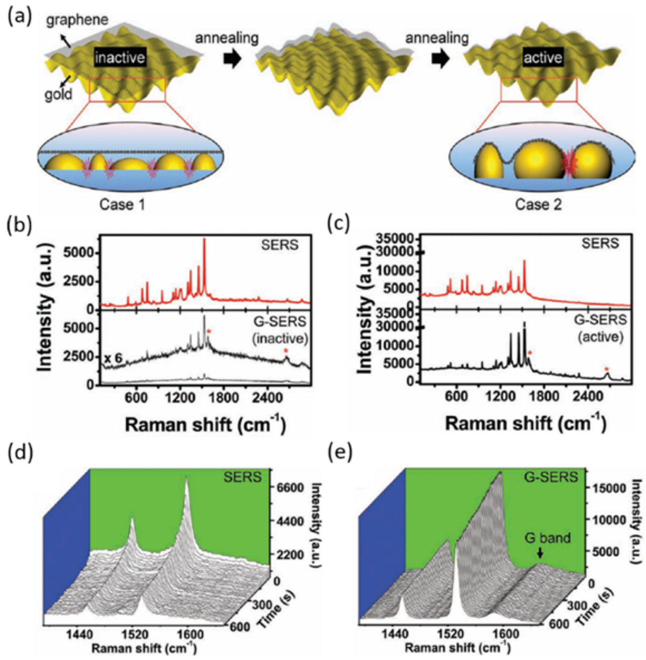

Figure 4. (a) Schematic illustration of graphene-veiled SERS substrates with graphene spread over the curved side of gold nanoislands before and after an activation process of thermal annealing. (b, c) SERS performance of normal SERS (top) and G-SERS regions (bottom) before (b) and after (c) annealing, respectively. "*" marks the G and G′ bands of the bilayer graphene (2LG). (d, e) Stability of the enhanced Raman signal of CuPc by normal SERS (d) and G-SERS (e) after thermal annealing activation. The peak at 1586 cm^{-1} in (e) is the G band of graphene. Adapted with permission from ref 74. Copyright 2013 John Wiley & Sons, Inc.

8 nm gold film with island-like structures, and a thermal annealing procedure was implemented to "activate" the SERS performance. Before annealing, graphene cannot extend to the nanogaps between particles, so that the molecules cannot be enhanced by the electromagnetic "hot spots".

By comparing the SERS performance of the regions with and without graphene before and after annealing (Figure 4b, c), respectively, it was observed that G-SERS tends to provide a greatly enhanced GERS signal comparable to SERS, yet keeping the pristine features of GERS. As the molecules are on the graphene surface and separated from metal, graphene-veiled SERS can enable enhanced Raman signals with improved reproducibility. As shown in Figure 4d and 4e, during a temporal measurement of 600 s, the intensity of the Raman signal of CuPc in the normal SERS region decreased quickly, while in the graphene-veiled region it remained stable.

Along this line, a series of similar work have also been reported. Liu et al. grew graphene with controlled layer numbers directly on the surface of metal nanoparticles via chemical vapor deposition, forming graphene-encapsulated metal nanoparticles (M@G, where M = Cu, Ag, and Au) for SERS.[75] Ultraviolet−visible spectroscopic measurements in-

DOI: 10.1021/acs.chemmater.6b02925
Chem. Mater. 2016, 28, 6426−6435

dicated that graphene can prevent the surface oxidation of metal nanoparticles exposed in ambient air, greatly elongating the lifetime of the metal nanoparticles for SERS. The Raman spectra of cobalt phthalocyanine (CoPc) and R6g on M@G substrates also showed that Au@G can dramatically suppress photobleaching and fluorescence of the probe molecules, resulting in a cleaner enhanced Raman signal that is suitable for sensing applications.

As graphene behaves superiorly in terms of biocompatibility and chemical stability, many methods toward graphene-veiled hybrid substrate, such as graphene covered gold nanocap arrays, graphene/Au nanopyramid hybrid structures, and Ag@GO hybrid,[76−79] have been developed in recent studies, especially for biosensing applications. For example, Kim et al. fabricated 3D graphene oxide (GO)-encapsulated gold nanoparticles to monitor the neural stem cell (NSC) differentiation, and undifferentiated stem cells were found to have many molecules that contain a high number of C═C bonds which are also highly adhesive to the surface of GO.[76] The Raman signals obtained from undifferentiated NSCs on the GO-encapsulated gold nanoparticles were 3.5 times higher than those from normal metal structures and can be clearly distinguished from those of differentiated cells, which provides a potential application as a nondestructive in situ monitoring tool for the identification of the differentiation potential of various kinds of stem cells. Wang et al. demonstrated a graphene−Au nanopyramids hybrid system with single-molecule sensitivity. This hybrid system benefits a much higher density of hot spots with EF of over 10^{10} for R6G as well as lysozyme (a kind of protein), and enables label-free sensing.[78]

Such structures have also been applied in quasi-quantitative applications. For example, Xu et al. fabricated graphene isolated Au nanoparticle arrays,[80] and detected the adenosine concentration in human serum with a good linear correlation between SERS intensity and adenosine concentration within the range of 2 to 250 nM. A hybrid structure of monolayer graphene and Cu nanoparticles was also used for adenosine detection with a reasonable linear response in the concentrations of 10^{-2}−10^{-6} M and the limit of detection down to 10^{-8} M.[81,82]

4.3. Pushing "Hot Spots" to the Flat Surface of Graphene. The graphene-veiled SERS ensures stable Raman signals and has been a big step forward for reliable sensing. However, the surface morphology replicates that of metal nanostructures and is of nanoscale roughness, so that it lacks the capability of an important application of sensing—SERS quantification. Recently, Gwo et al. showed that the EM enhancement is nearly homogeneous on the flat surface of a thin layer of polymer on close-packed metal nanoparticles,[83] which holds potential for SERS quantification. By virtue of the 2D crystalline nature of graphene, we developed a G-SERS substrate with atomic flatness. As illustrated in Figure 5a, a monolayer graphene (1LG) with gold/silver nanoislands was tightly adhered on the backside.[84] The section analysis of the atomic force microscopy (AFM) image indicates that the surface of the resulting G-SERS substrate has a height fluctuation of less than ±2 nm. The electromagnetic "hot spots" created by the gapped metal nanoislands through the localized surface plasmon resonance can penetrate the monolayer graphene, resulting in an atomically flat "hot surface" for Raman enhancement. This surface has the EM enhancement by gold or silver nanoislands adhered on the backside of graphene and, more importantly, renders control-

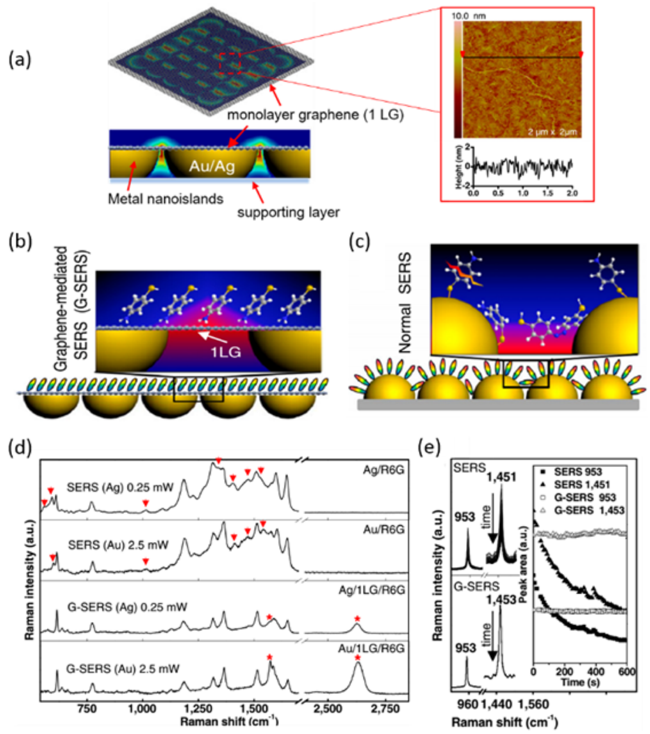

Figure 5. (a) Design of a flat G-SERS substrate. The inset is the atomic force microscopy (AFM) image of the graphene side of a G-SERS(Au) tape (top), together with a section analysis on the bottom. (b, c) Schematic illustration of molecules adsorbed on a flat G-SERS substrate (b) and on a normal SERS substrate (c). (d) SERS and G-SERS spectra of R6G with gold and silver nanoislands used as an electromagnetic enhancer, respectively. Red arrows point to the additional and nonreproducible peaks in the spectra of normal SERS. (e) Stability of the SERS (top) and G-SERS (bottom) spectra of CuPc in a time series of 600 s. The inset shows the integrated intensity of the peaks change with the increase of time. Adapted with permission from ref 84. Copyright 2012 National Academy of Sciences.

lable molecular arrangements as well as well-defined molecular interactions (Figure 5b, c).

As shown in Figure 5d, the flat G-SERS substrates showed highly consistent results for R6G with gold or silver as the electromagnetic enhancer, while some irreproducible shifted or new-emerging features were observed with bare gold or silver SERS substrate.

Apart from the cleaner vibrational features and higher stability against photoinduced damage, the flat G-SERS substrate maintains a comparable EF to those of normal SERS substrates. SERS spectra of CuPc with pristine, GERS, G-SERS(Au), SERS(Au), G-SERS(Ag), and SERS(Ag) substrates, respectively, were measured under the same conditions. The pristine intensity of the 1530 cm^{-1} peak was enhanced by a factor of 14 for GERS, 61 for SERS (Au), 85 for G-SERS (Au), 580 for SERS (Ag), and 755 for G-SERS (Ag). These results showed that the flat G-SERS is capable of ultrasensitive detection with comparable (and even larger, for certain vibrational modes) enhancement to that of normal SERS using the same metal nanostructures.

Another feature toward sensing application is again the stability of the Raman spectra. As shown in Figure 5e, in the flat G-SERS system, the Raman signal of CuPc remained totally stable with the intervention of graphene, while in the normal SERS region it decreased quickly in intensity during a 600 s

DOI: 10.1021/acs.chemmater.6b02925
Chem. Mater. 2016, 28, 6426−6435

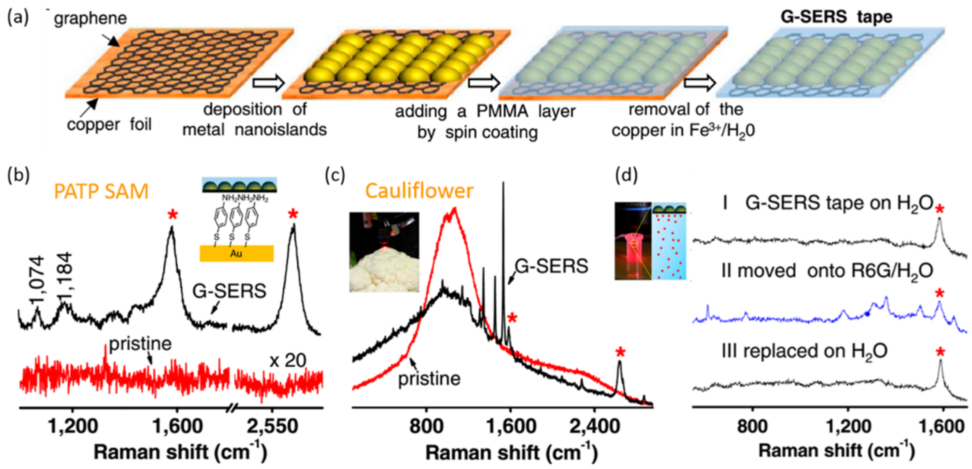

Figure 6. (a) Schematic of the preparation route of the transparent, freestanding, and flexible G-SERS tape from CVD-grown monolayer graphene. (b) Pristine (red line) and G-SERS (black line) measurements of a self-assembled monolayer of *p*-aminothiophenol on a flat gold surface. (c) Pristine (red line) and G-SERS (black line) spectra of a cauliflower surface with adsorbed CuPc (by soaking in a 1×10^{-5} M CuPc solution in ethanol for 10 min). (d) A real time and reversible G-SERS characterization of R6G directly in a 1×10^{-5} M aqueous solution. (I, II, and III are the Raman spectra with the same G-SERS tape on H_2O, $R6G/H_2O$, and replaced on H_2O, respectively.) Adapted with permission from ref 84.

measurement. It is speculated that both the separation of CuPc from the rough gold film and the formation of a graphene/CuPc complex through $\pi-\pi$ interactions may contribute to the stability of CuPc.

In the flat G-SERS substrates, graphene contributes multi-functions toward sensing: a spacer for surface passivation, a fluorescence quencher, and an additional chemical enhancer. The atomic thickness, the seamless structure, and the chemical inertness of graphene isolate the undesirable interactions between molecules and metal, promising cleaner, more reproducible, and ultrahigh sensitive SERS signals. In addition, graphene can also enrich aromatic analytes through $\pi-\pi$ interaction, which may decrease the limit of detection.

5. G-SERS TAPE TOWARD PRACTICAL ANALYTICAL APPLICATIONS

5.1. Transparent, Flexible, and Freestanding G-SERS Tape. It is an incessant goal all along to enable direct, real time, and reliable detection of trace amounts of analytes in various systems. In order to promote the analytical applications of SERS in daily life, a flexible and universal substrate is needed to satisfy the in situ detection on an arbitrary surface. To this end, we developed transparent, flexible, and free-standing G-SERS tapes for arbitrary surface detection.[84] The fabrication process is shown in Figure 6a. First an 8 nm gold/silver film was deposited on a uniform CVD-grown monolayer graphene of large area and high quality, and then a poly(methyl methacrylate) (PMMA) film (which is optically transparent, inert, and Raman inactive) was fabricated on top, and finally the copper foil underneath was etched by a $FeCl_3/H_2O$ solution. This fabrication technique is suitable for scalable production of G-SERS tapes.

In this so-called G-SERS tape, graphene serves as the molecule/nanoparticle spacer and supplies a clean and atomically smooth surface for the adsorption of target molecules, and the 8 nm gold film provides the indispensable electromagnetic enhancement. Particularly, owing to the transparent and flexible properties, the PMMA film is a superior candidate as the support layer, with which the G-SERS substrate can float on an aqueous solution for the in situ Raman detection, or stick onto any surface with arbitrary morphology for the detection of a trace amount molecules.

Figure 6(b−d) demonstrated three examples of real-time detection using G-SERS. The Raman spectra of a self-assembled monolayer of *p*-aminothiophenol on a flat gold surface (Figure 6b) and of CuPc molecules adsorbed on a cauliflower surface (Figure 6c) were successfully obtained, which indicates the universality of our G-SERS tape.

G-SERS tape can also be used directly in an aqueous solution for real-time analysis (Figure 6d). We can get the intrinsic Raman signal of R6G with a clear graphene signal as internal reference. Additionally, the R6G signal disappeared after washing and replacing the G-SERS tape on water. This reversibility suggests that G-SERS tape is reusable with no residues. It is beneficial in real time sensing processes, such as online monitoring of water contaminants.

5.2. In Situ Quantitative Analysis. So far, several approaches have been developed aiming at reliable quantitative SERS analysis with high resolution and sensitivity, for example, the implementation of internal standards and the univariate and multivariate data analysis method.[83,85,86] The main problems that hinder the practical SERS quantification include the Raman signal fluctuation and the uncertainty of the amount of detected molecules. The former can be overcome by the direct use of graphene as a spacer that separates the molecules and metal. The latter is also possible to be resolved by using G-SERS tape, where the 2D single-crystalline nature of graphene promises the homogeneous adsorption of molecules to ensure the number of molecules. Besides, the characteristic Raman feature of graphene can serve as an internal standard (IS) for the calibration of SERS intensities, which can effectively eliminate the signal fluctuation and the influence of the nonuniform distribution of hot spots, promising reliable quantitative SERS analysis of target molecules with different affinities to the surface. Our data has shown the in situ quantification of probe molecules, such as crystal violet, in aqueous solutions down to the detection limit of 10^{-8} mol/L. The Raman intensities can be plotted as a function of concentration, and the Langmuir isothermal model can be used to fit the curve, from which the adsorption constant and surface coverage of the analyte

DOI: 10.1021/acs.chemmater.6b02925
Chem. Mater. 2016, 28, 6426−6435

molecules on graphene can be obtained. Such information is essential for SERS quantification of unknown concentrations.

6. CONCLUSION AND OUTLOOK

In this review, we introduced the progress of SERS using graphene and other diverse 2D layered materials as the substrate. The chemical enhancement by graphene and other 2D materials was reviewed, and the role of in-plane symmetry was also discussed in the case of anisotropic 2D materials. This not only renders deeper understanding of the CM process in SERS, but also lights up the possibility of the symmetry dependent SERS sensing. From the analytical application point of view, the advantages incurred by graphene, including clean signal, stable response, intrinsic inertial reference, flexibility, and recyclability, enable G-SERS as a more desirable analytical tool for sensing. More importantly, the G-SERS tape can be used on an arbitrary surface, and is proven promising for highly sensitive and reliable in situ quantitative analysis.

From the fundamental point of view, graphene-based SERS is relatively clearer. The chemical process in G-SERS has been systematically explored, and more attention has been paid to the application aspect. Nevertheless, doped-graphene as a SERS substrate may reveal more information on the energy alignment aspect. On the other hand, other 2D materials enhanced Raman scattering is more challenging. For example, the energy band structures of the materials are usually sensitive to the number of layers; the charge interaction can also depend on the molecular orientation with respect to the in-plane crystalline directions; and the stability of the 2D materials under ambient conditions is an important issue to consider for reliable measurements. Regardless of these challenges, the extension of substrates to more 2D materials is still necessary in order to further explore the charge interactions and the CM of SERS, and more detailed studies using more sophisticated techniques, such as ultrafast optical measurements, are required.

From the analytical application point of view, SERS quantification is one of the most useful directions. A robust SERS quantification method with wide linear range and high precision is still in demand. In situ quantitative detection using G-SERS is promising due to not only the characteristic features of graphene as mentioned above, but also the flexibility and transparency of the graphene-based polymer supported substrate. In this topical area, future directions are apparent: first, the improvement of the enhancement factor by the optimization of metal nanostructures and/or the functionalization of graphene is a must. This allows a much higher sensitivity and wider linear-response range of concentration. Second, a reliable model for the specific detection of one species in multicomponent systems is urgent, because in almost all the practical cases, the systems to be analyzed contain multiple components. Third, the reliable demonstration of the practical application of the in situ quantitation using G-SERS tape is necessary, for example, in the detection of food additives in a food market. This is certainly the ultimate goal to pursue, and we believe that this review article will find its place along this line.

AUTHOR INFORMATION

Corresponding Authors

*E-mail: tonglm@pku.edu.cn.
*E-mail: jinzhang@pku.edu.cn.

Notes

The authors declare no competing financial interest.

ACKNOWLEDGMENTS

J.Z. and L.T. acknowledge funding from NSFC (21233001, 21129001, 51272006, 51432002, 51121091, 11374355, and 21573004) and MOST (2016YFA0200101 and 2016YFA0200104).

ABBREVIATIONS

SERS, surface-enhanced Raman spectroscopy; GERS, graphene-enhanced Raman scattering; G-SERS, graphene-based surface-enhanced Raman scattering; EM, electromagnetic mechanism; CM, chemical mechanism; EF, enhancement factor

REFERENCES

(1) Fleischmann, M.; Hendra, P. J.; McQuillan, A. Raman spectra of pyridine adsorbed at a silver electrode. *Chem. Phys. Lett.* **1974**, *26* (2), 163−166.

(2) Campion, A.; Kambhampati, P. Surface-enhanced Raman scattering. *Chem. Soc. Rev.* **1998**, *27* (4), 241−250.

(3) Tian, Z. Q. Surface-enhanced Raman spectroscopy: advancements and applications. *J. Raman Spectrosc.* **2005**, *36* (6−7), 466−470.

(4) Sharma, B.; Frontiera, R. R.; Henry, A.-I.; Ringe, E.; Van Duyne, R. P. SERS: Materials, applications, and the future. *Mater. Today* **2012**, *15* (1−2), 16−25.

(5) Schluecker, S. Surface-enhanced Raman spectroscopy: concepts and chemical applications. *Angew. Chem., Int. Ed.* **2014**, *53* (19), 4756−4795.

(6) Otto, A.; Mrozek, I.; Grabhorn, H.; Akemann, W. Surface-enhanced Raman scattering. *J. Phys.: Condens. Matter* **1992**, *4* (5), 1143.

(7) Moskovits, M. Surface-enhanced spectroscopy. *Rev. Mod. Phys.* **1985**, *57* (3), 783.

(8) Otto, A. The 'chemical' (electronic) contribution to surface-enhanced Raman scattering. *J. Raman Spectrosc.* **2005**, *36* (6−7), 497−509.

(9) Schatz, G. C.; Young, M. A.; Van Duyne, R. P. Electromagnetic mechanism of SERS. In *Surface-enhanced Raman scattering*; Springer: 2006; pp 19−45.

(10) Le Ru, E.; Etchegoin, P. *Principles of surface-enhanced Raman spectroscopy: and related plasmonic effects*; Elsevier: 2008.

(11) Käll, M.; Xu, H.; Johansson, P. Field enhancement and molecular response in surface-enhanced Raman scattering and fluorescence spectroscopy. *J. Raman Spectrosc.* **2005**, *36* (6−7), 510−514.

(12) Persson, B. N. J.; Zhao, K.; Zhang, Z. Chemical contribution to surface-enhanced Raman scattering. *Phys. Rev. Lett.* **2006**, *96* (20), 207401.

(13) Kneipp, K.; Wang, Y.; Kneipp, H.; Perelman, L. T.; Itzkan, I.; Dasari, R. R.; Feld, M. S. Single molecule detection using surface-enhanced Raman scattering (SERS). *Phys. Rev. Lett.* **1997**, *78* (9), 1667.

(14) Nie, S.; Emory, S. R. Probing single molecules and single nanoparticles by surface-enhanced Raman scattering. *Science* **1997**, *275* (5303), 1102−1106.

(15) Huang, Y. F.; Zhu, H. P.; Liu, G. K.; Wu, D. Y.; Ren, B.; Tian, Z. Q. When the signal is not from the original molecule to be detected: chemical transformation of para-aminothiophenol on Ag during the SERS measurement. *J. Am. Chem. Soc.* **2010**, *132* (27), 9244−9246.

(16) Li, J. F.; Huang, Y. F.; Ding, Y.; Yang, Z. L.; Li, S. B.; Zhou, X. S.; Fan, F. R.; Zhang, W.; Zhou, Z. Y.; Ren, B.; Wang, Z. L.; Tian, Z. Q. Shell-isolated nanoparticle-enhanced Raman spectroscopy. *Nature* **2010**, *464* (7287), 392−395.

(17) Novoselov, K. S.; Geim, A. K.; Morozov, S. V.; Jiang, D.; Zhang, Y.; Dubonos, S. V.; Grigorieva, I. V.; Firsov, A. A. Electric field effect in atomically thin carbon films. *Science* **2004**, *306* (5696), 666−669.

DOI: 10.1021/acs.chemmater.6b02925
Chem. Mater. 2016, 28, 6426−6435

(18) Schedin, F.; Geim, A.; Morozov, S.; Hill, E.; Blake, P.; Katsnelson, M.; Novoselov, K. Detection of individual gas molecules adsorbed on graphene. *Nat. Mater.* **2007**, *6* (9), 652−655.
(19) Berger, C.; Song, Z.; Li, T.; Li, X.; Ogbazghi, A. Y.; Feng, R.; Dai, Z.; Marchenkov, A. N.; Conrad, E. H.; First, P. N.; De Heer, W. A. Ultrathin epitaxial graphite: 2D electron gas properties and a route toward graphene-based nanoelectronics. *J. Phys. Chem. B* **2004**, *108* (52), 19912−19916.
(20) Huang, X.; Zeng, Z.; Fan, Z.; Liu, J.; Zhang, H. Graphene-based electrodes. *Adv. Mater.* **2012**, *24* (45), 5979−6004.
(21) He, Q.; Wu, S.; Yin, Z.; Zhang, H. Graphene-based electronic sensors. *Chem. Sci.* **2012**, *3* (6), 1764−1772.
(22) Cao, X.; Zeng, Z.; Shi, W.; Yep, P.; Yan, Q.; Zhang, H. Three-Dimensional Graphene Network Composites for Detection of Hydrogen Peroxide. *Small* **2013**, *9* (9−10), 1703−1707.
(23) Wu, S.; He, Q.; Tan, C.; Wang, Y.; Zhang, H. Graphene-Based Electrochemical Sensors. *Small* **2013**, *9* (8), 1160−1172.
(24) Geim, A. K.; Novoselov, K. S. The rise of graphene. *Nat. Mater.* **2007**, *6* (3), 183−191.
(25) Geim, A. K. Graphene: status and prospects. *Science* **2009**, *324* (5934), 1530−1534.
(26) Casiraghi, C.; Hartschuh, A.; Lidorikis, E.; Qian, H.; Harutyunyan, H.; Gokus, T.; Novoselov, K.; Ferrari, A. Rayleigh imaging of graphene and graphene layers. *Nano Lett.* **2007**, *7* (9), 2711−2717.
(27) Abergel, D. S. L.; Russell, A.; Fal'ko, V. I. Visibility of graphene flakes on a dielectric substrate. *Appl. Phys. Lett.* **2007**, *91*, 063125.
(28) Blake, P.; Hill, E.; Neto, A. C.; Novoselov, K.; Jiang, D.; Yang, R.; Booth, T.; Geim, A. Making graphene visible. *Appl. Phys. Lett.* **2007**, *91* (6), 063124.
(29) Ling, X.; Xie, L.; Fang, Y.; Xu, H.; Zhang, H.; Kong, J.; Dresselhaus, M. S.; Zhang, J.; Liu, Z. Can graphene be used as a substrate for Raman enhancement? *Nano Lett.* **2010**, *10* (2), 553−561.
(30) Xu, W.; Mao, N.; Zhang, J. Graphene: A platform for surface-enhanced Raman spectroscopy. *Small* **2013**, *9* (8), 1206−1224.
(31) Kang, L.; Chu, J.; Zhao, H.; Xu, P.; Sun, M. Recent progress in the applications of graphene in surface-enhanced Raman scattering and plasmon-induced catalytic reactions. *J. Mater. Chem. C* **2015**, *3* (35), 9024−9037.
(32) Ling, X.; Huang, S.; Deng, S.; Mao, N.; Kong, J.; Dresselhaus, M. S.; Zhang, J. Lighting up the Raman signal of molecules in the vicinity of graphene related materials. *Acc. Chem. Res.* **2015**, *48* (7), 1862−1870.
(33) Xu, Y. Y.; Yang, C.; Jiang, S. Z.; Man, B. Y.; Liu, M.; Chen, C. S.; Zhang, C.; Sun, Z. C.; Qiu, H. W.; Li, H. S.; Feng, D. J.; Zhang, J. X. Layer-controlled large area MoS2 layers grown on mica substrate for surface-enhanced Raman scattering. *Appl. Surf. Sci.* **2015**, *357*, 1708−1713.
(34) Qiu, H.; Li, Z.; Gao, S.; Chen, P.; Zhang, C.; Jiang, S.; Xu, S.; Yang, C.; Li, H. Large-area MoS_2 thin layers directly synthesized on Pyramid-Si substrate for surface-enhanced Raman scattering. *RSC Adv.* **2015**, *5* (102), 83899−83905.
(35) Ling, X.; Fang, W.; Lee, Y.-H.; Araujo, P. T.; Zhang, X.; Rodriguez-Nieva, J. F.; Lin, Y.; Zhang, J.; Kong, J.; Dresselhaus, M. S. Raman enhancement effect on two-dimensional layered materials: graphene, h-BN and MoS_2. *Nano Lett.* **2014**, *14* (6), 3033−3040.
(36) Lee, Y.; Kim, H.; Lee, J.; Yu, S. H.; Hwang, E.; Lee, C.; Ahn, J.-H.; Cho, J. H. Enhanced Raman scattering of Rhodamine 6G films on two-dimensional transition metal dichalcogenides correlated to photoinduced charge transfer. *Chem. Mater.* **2016**, *28* (1), 180−187.
(37) Lin, J.; Liang, L.; Ling, X.; Zhang, S.; Mao, N.; Zhang, N.; Sumpter, B. G.; Meunier, V.; Tong, L.; Zhang, J. Enhanced Raman scattering on in-plane anisotropic layered materials. *J. Am. Chem. Soc.* **2015**, *137* (49), 15511−15517.
(38) Liu, M.; Zhao, H.; Quan, X.; Chen, S.; Fan, X. Distance-independent quenching of quantum dots by nanoscale-graphene in self-assembled sandwich immunoassay. *Chem. Commun.* **2010**, *46* (42), 7909−7911.
(39) Xie, L.; Ling, X.; Fang, Y.; Zhang, J.; Liu, Z. Graphene as a substrate to suppress fluorescence in resonance Raman spectroscopy. *J. Am. Chem. Soc.* **2009**, *131* (29), 9890−9891.
(40) Swathi, R.; Sebastian, K. Resonance energy transfer from a dye molecule to graphene. *J. Chem. Phys.* **2008**, *129* (5), 054703.
(41) Ling, X.; Zhang, J. First-layer effect in graphene-enhanced Raman scattering. *Small* **2010**, *6* (18), 2020−2025.
(42) Ling, X.; Wu, J.; Xu, W.; Zhang, J. Probing the Effect of molecular orientation on the intensity of chemical enhancement using graphene-enhanced Raman spectroscopy. *Small* **2012**, *8* (9), 1365−1372.
(43) Xu, H.; Chen, Y.; Xu, W.; Zhang, H.; Kong, J.; Dresselhaus, M. S.; Zhang, J. Modulating the charge-transfer enhancement in GERS using an electrical field under vacuum and an n/p-doping atmosphere. *Small* **2011**, *7* (20), 2945−2952.
(44) Xu, H.; Xie, L.; Zhang, H.; Zhang, J. Effect of graphene fermi level on the Raman scattering intensity of molecules on graphene. *ACS Nano* **2011**, *5* (7), 5338−5344.
(45) Ling, X.; Moura, L. G.; Pimenta, M. A.; Zhang, J. Charge-transfer mechanism in graphene-enhanced Raman scattering. *J. Phys. Chem. C* **2012**, *116* (47), 25112−25118.
(46) Ling, X.; Wu, J.; Xie, L.; Zhang, J. Graphene-thickness-dependent graphene-enhanced Raman scattering. *J. Phys. Chem. C* **2013**, *117* (5), 2369−2376.
(47) Quan, L.; Song, Y.; Lin, Y.; Zhang, G.; Dai, Y.; Wu, Y.; Jin, K.; Ding, H.; Pan, N.; Luo, Y.; Wang, X. The Raman enhancement effect on a thin GaSe flake and its thickness dependence. *J. Mater. Chem. C* **2015**, *3* (42), 11129−11134.
(48) Xia, F.; Wang, H.; Jia, Y., Rediscovering black phosphorus as an anisotropic layered material for optoelectronics and electronics. *Nat. Commun.* **2014**, *5*, 10.1038/ncomms5458
(49) Liu, H.; Neal, A. T.; Zhu, Z.; Luo, Z.; Xu, X.; Tománek, D.; Ye, P. D. Phosphorene: an unexplored 2D semiconductor with a high hole mobility. *ACS Nano* **2014**, *8* (4), 4033−4041.
(50) Morita, A. Semiconducting black phosphorus. *Appl. Phys. A: Solids Surf.* **1986**, *39* (4), 227−242.
(51) Wu, J.; Mao, N.; Xie, L.; Xu, H.; Zhang, J. Identifying the crystalline orientation of black phosphorus using angle-resolved polarized Raman spectroscopy. *Angew. Chem.* **2015**, *127* (8), 2396−2399.
(52) Kneipp, K.; Kneipp, H.; Itzkan, I.; Dasari, R. R.; Feld, M. S. Ultrasensitive chemical analysis by Raman spectroscopy. *Chem. Rev.* **1999**, *99* (10), 2957−2976.
(53) Michaels, A. M.; Nirmal, M.; Brus, L. Surface enhanced Raman spectroscopy of individual rhodamine 6G molecules on large Ag nanocrystals. *J. Am. Chem. Soc.* **1999**, *121* (43), 9932−9939.
(54) Geick, R.; Perry, C.; Rupprecht, G. Normal modes in hexagonal boron nitride. *Phys. Rev.* **1966**, *146* (2), 543.
(55) Lin, Y.; Bunker, C. E.; Fernando, K. S.; Connell, J. W. Aqueously dispersed silver nanoparticle-decorated boron nitride nanosheets for reusable, thermal oxidation-resistant surface enhanced Raman spectroscopy (SERS) devices. *ACS Appl. Mater. Interfaces* **2012**, *4* (2), 1110−1117.
(56) Yang, S.; Zhang, Z.; Zhao, J.; Zheng, H. High surface enhanced Raman scattering activity of BN nanosheets−Ag nanoparticles hybrids. *J. Alloys Compd.* **2014**, *583*, 231−236.
(57) Huang, J.; Zhang, L.; Chen, B.; Ji, N.; Chen, F.; Zhang, Y.; Zhang, Z. Nanocomposites of size-controlled gold nanoparticles and graphene oxide: Formation and applications in SERS and catalysis. *Nanoscale* **2010**, *2*, 2733−2738.
(58) Chen, P.; Yin, Z.; Huang, X.; Wu, S.; Liedberg, B.; Zhang, H. Assembly of graphene oxide and $Au_{0.7}Ag_{0.3}$ alloy nanoparticles on SiO_2: a new Raman substrate with ultrahigh signal-to-background ratio. *J. Phys. Chem. C* **2011**, *115* (49), 24080−24084.
(59) Lu, G.; Li, H.; Liusman, C.; Yin, Z.; Wu, S.; Zhang, H. Surface enhanced Raman scattering of Ag or Au nanoparticle-decorated reduced graphene oxide for detection of aromatic molecules. *Chem. Sci.* **2011**, *2* (9), 1817−1821.

DOI: 10.1021/acs.chemmater.6b02925
Chem. Mater. 2016, 28, 6426−6435

(60) Zhao, H.; Fu, H.; Zhao, T.; Wang, L.; Tan, T. Fabrication of small-sized silver NPs/graphene sheets for high-quality surface-enhanced Raman scattering. *J. Colloid Interface Sci.* **2012**, *375*, 30−34.
(61) Hu, C.; Rong, J.; Cui, J.; Yang, Y.; Yang, L.; Wang, Y.; Liu, Y. Fabrication of a graphene oxide-gold nanorod hybrid material by electrostatic self-assembly for surface-enhanced Raman scattering. *Carbon* **2013**, *51*, 255−264.
(62) Kim, H.; Seol, M.-L.; Lee, D.-I.; Lee, J.; Kang, I.-S.; Lee, H.; Kang, T.; Choi, Y.-K.; Kim, B. Single nanowire on graphene (SNOG) as an efficient, reproducible, and stable SERS-active platform. *Nanoscale* **2016**, *8* (16), 8886−8894.
(63) Leem, J.; Wang, M. C.; Kang, P.; Nam, S. Mechanically Self-Assembled, Three-Dimensional Graphene-Gold Hybrid Nanostructures for Advanced Nanoplasmonic Sensors. *Nano Lett.* **2015**, *15* (11), 7684−7690.
(64) Yin, P. T.; Kim, T.-H.; Choi, J.-W.; Lee, K.-B. Prospects for graphene-nanoparticle-based hybrid sensors. *Phys. Chem. Chem. Phys.* **2013**, *15* (31), 12785−12799.
(65) Zhang, L.; Jiang, C.; Zhang, Z. Graphene oxide embedded sandwich nanostructures for enhanced Raman readout and their applications in pesticide monitoring. *Nanoscale* **2013**, *5* (9), 3773−3779.
(66) Liu, X.; Cao, L.; Song, W.; Ai, K.; Lu, L. Functionalizing Metal Nanostructured Film with Graphene Oxide for Ultrasensitive Detection of Aromatic Molecules by Surface-Enhanced Raman Spectroscopy. *ACS Appl. Mater. Interfaces* **2011**, *3* (8), 2944−2952.
(67) Lu, G.; Li, H.; Liusman, C.; Yin, Z.; Wu, S.; Zhang, H. Surface enhanced Raman scattering of Ag or Au nanoparticle-decorated reduced graphene oxide for detection of aromatic molecules. *Chem. Sci.* **2011**, *2* (9), 1817−1821.
(68) Dutta, S.; Ray, C.; Sarkar, S.; Pradhan, M.; Negishi, Y.; Pal, T. Silver Nanoparticle Decorated Reduced Graphene Oxide (rGO) Nanosheet: A Platform for SERS Based Low-Level Detection of Uranyl Ion. *ACS Appl. Mater. Interfaces* **2013**, *5* (17), 8724−8732.
(69) He, S.; Liu, K.-K.; Su, S.; Yan, J.; Mao, X.; Wang, D.; He, Y.; Li, L.-J.; Song, S.; Fan, C. Graphene-Based High-Efficiency Surface-Enhanced Raman Scattering-Active Platform for Sensitive and Multiplex DNA Detection. *Anal. Chem.* **2012**, *84* (10), 4622−4627.
(70) Fan, Z.; Kanchanapally, R.; Ray, P. C. Hybrid Graphene Oxide Based Ultrasensitive SERS Probe for Label-Free Biosensing. *J. Phys. Chem. Lett.* **2013**, *4* (21), 3813−3818.
(71) Kanchanapally, R.; Sinha, S. S.; Fan, Z.; Dubey, M.; Zakar, E.; Ray, P. C. Graphene Oxide-Gold Nanocage Hybrid Platform for Trace Level Identification of Nitro Explosives Using a Raman Fingerprint. *J. Phys. Chem. C* **2014**, *118* (13), 7070−7075.
(72) Lu, R.; Konzelmann, A.; Xu, F.; Gong, Y.; Liu, J.; Liu, Q.; Xin, M.; Hui, R.; Wu, J. Z. High sensitivity surface enhanced Raman spectroscopy of R6G on in situ fabricated Au nanoparticle/graphene plasmonic substrates. *Carbon* **2015**, *86*, 78−85.
(73) Li, J. F.; Tian, X. D.; Li, S. B.; Anema, J. R.; Yang, Z. L.; Ding, Y.; Wu, Y. F.; Zeng, Y. M.; Chen, Q. Z.; Ren, B.; Wang, Z. L.; Tian, Z. Q. Surface analysis using shell-isolated nanoparticle-enhanced Raman spectroscopy. *Nat. Protoc.* **2013**, *8* (1), 52−65.
(74) Xu, W.; Xiao, J.; Chen, Y.; Chen, Y.; Ling, X.; Zhang, J. Graphene-veiled gold substrate for surface-enhanced Raman spectroscopy. *Adv. Mater.* **2013**, *25* (6), 928−933.
(75) Liu, Y.; Hu, Y.; Zhang, J. Few-layer graphene-encapsulated metal nanoparticles for surface-enhanced Raman spectroscopy. *J. Phys. Chem. C* **2014**, *118* (17), 8993−8998.
(76) Kim, T.-H.; Lee, K.-B.; Choi, J.-W. 3D graphene oxide-encapsulated gold nanoparticles to detect neural stem cell differentiation. *Biomaterials* **2013**, *34* (34), 8660−8670.
(77) Long, K.; Luo, X.; Nan, H.; Du, D.; Zhao, W.; Ni, Z.; Qiu, T. Surface-enhanced Raman scattering from graphene covered gold nanocap arrays. *J. Appl. Phys.* **2013**, *114*, 183520.
(78) Wang, P.; Liang, O.; Zhang, W.; Schroeder, T.; Xie, Y.-H. Ultra-sensitive graphene-plasmonic hybrid platform for label-free detection. *Adv. Mater.* **2013**, *25* (35), 4918−4924.
(79) Chen, S.; Li, X.; Zhao, Y.; Chang, L.; Qi, J. Graphene oxide shell-isolated Ag nanoparticles for surface-enhanced Raman scattering. *Carbon* **2015**, *81*, 767−772.
(80) Xu, S.; Jiang, S.; Wang, J.; Wei, J.; Yue, W.; Ma, Y. Graphene isolated Au nanoparticle arrays with high reproducibility for high-performance surface-enhanced Raman scattering. *Sens. Actuators, B* **2016**, *222*, 1175−1183.
(81) Qiu, H.; Huo, Y.; Li, Z.; Zhang, C.; Chen, P.; Jiang, S.; Xu, S.; Ma, Y.; Wang, S.; Li, H. Surface-enhanced Raman scattering based on controllable-layer graphene shells directly synthesized on Cu nanoparticles for molecular detection. *ChemPhysChem* **2015**, *16* (14), 2953−2960.
(82) Qiu, H. W.; Xu, S. C.; Chen, P. X.; Gao, S. S.; Li, Z.; Zhang, C.; Jiang, S. Z.; Liu, M.; Li, H. S.; Feng, D. J. A novel surface-enhanced Raman spectroscopy substrate based on hybrid structure of monolayer graphene and Cu nanoparticles for adenosine detection. *Appl. Surf. Sci.* **2015**, *332*, 614−619.
(83) Chen, H.-Y.; Lin, M.-H.; Wang, C.-Y.; Chang, Y.-M.; Gwo, S. Large-scale hot spot engineering for quantitative SERS at the single-molecule scale. *J. Am. Chem. Soc.* **2015**, *137* (42), 13698−13705.
(84) Xu, W.; Ling, X.; Xiao, J.; Dresselhaus, M. S.; Kong, J.; Xu, H.; Liu, Z.; Zhang, J. Surface enhanced Raman spectroscopy on a flat graphene surface. *Proc. Natl. Acad. Sci. U. S. A.* **2012**, *109* (24), 9281−9286.
(85) Bell, S. E.; Sirimuthu, N. M. Quantitative surface-enhanced Raman spectroscopy. *Chem. Soc. Rev.* **2008**, *37* (5), 1012−1024.
(86) Shen, W.; Lin, X.; Jiang, C. Y.; Li, C.; Lin, H. X.; Huang, J. G.; Wang, S.; Liu, G. K.; Yan, X. M.; Zhong, Q. L.; Ren, B. Reliable quantitative SERS analysis facilitated by core−shell nanoparticles with embedded internal standards. *Angew. Chem.* **2015**, *127* (25), 7416−7420.

DOI: 10.1021/acs.chemmater.6b02925
Chem. Mater. 2016, 28, 6426−6435